Dynamic Modeling and Centralized Formation Control of Mobile Robots

Celso De La Cruz
Instituto de Automática (INAUT)
Universidad Nacional de San Juan (UNSJ)
1109 Libertador San Martín street (west)
J5400ARL, ARGENTINA
delacruz@inaut.unsj.edu.ar

Ricardo Carelli
Instituto de Automática (INAUT)
Universidad Nacional de San Juan (UNSJ)
1109 Libertador San Martín street (west)
J5400ARL, ARGENTINA
rcarelli@inaut.unsj.edu.ar

Abstract –**The work presents, first, a complete dynamic model of a unicycle-like mobile robot that takes part in a multi-robot formation. A linear parameterization of the model is also performed. The resulting robot model is input-output feedback linearized. On a second stage, for the multi-robot system, a model is obtained by arranging into a single equation all the feedback linearized robot models. This multi-robot model is expressed in terms of formation states by applying a coordinate transformation. The inverse dynamics technique is then applied to design a centralized formation control. The controller can be applied both to positioning and to tracking desired robot formations. Experimental results validate the theoretical aspects.**

Index Terms – Formation control, dynamic model, non-holonomic mobile robots, nonlinear systems.

I. INTRODUCTION

A marked trend in robot applications is calling for controlling coordinately a group of robots assigned to perform a specific task. The motivation for coordinated control lies on the fact that there are tasks which are impossible to perform with just one robot, and other tasks in which working with a number of robots is less expensive than with just one specialized robot. Examples of such tasks are: surveillance operations, search and exploration, rescue, survey and mapping, cooperative handling of objects, and others. Many of these applications need a formation control to perform the task efficiently.

Formation control strategies can be classified as centralized [10] when there is a monitoring and control of all robots by a central processor; or decentralized [17] when there is no supervisor, every robot has its own controller and the control feedback is only the detected relative positions of each robot respecting their neighbor robots.

Basically, there are three approaches for robot coordination reported in the literature: leader tracking [12], [7], behavior methods [9], [3], and virtual structure techniques [4], [16]. Most of the proposed coordination control systems are not based on dynamic systems and control theory, largely on account of the complexity of multi-robot systems. However, in order to ensure system stability, it is necessary to resort to using the tools from control theory and dynamic systems. For example in [11], the dynamic model of the mobile robot is output feedback linearized and the formation control is designed using passivity techniques, even though the control is based on a sequence of formations and not on a continuous tracking, and the control actions are forces and torques which are not simple to apply to real actuators. In [6], an input-output feedback linearization controller is designed and a switching strategy is used to control formations, although there is a constraint in that the leader velocity is bounded away from zero. In [10], a centralized formation control is proposed to manage omnidirectional robots; the stability of the resulting control system is proved by using Lyapunov theory.

In [1] and [15] the objective is to control the values taken by some *task functions* or *platoon-level functions*, such as the average position of the vehicles in a platoon or the distribution of the vehicles about the average position. In the present work these values are called formation states. In [1] a kinematic control of a platoon of autonomous vehicles was presented. In [15] a decentralized control system with minimum inter-vehicle communication was investigated, this control is based on a dynamic model linearized at an equilibrium value.

In this paper, a complete dynamic model of a unicycle-like mobile robot is developed in which the translational and rotational reference velocities are considered as the input signals. These signals are usual inputs in commercial robots. A linear parameterization of this robot model is also presented. The model is then input-output feedback linearized. The multi-robot system model is obtained by arranging into a single equation all the feedback linearized robot models. Initially, this multi-robot model is expressed in terms of absolute positions and linear velocities of the robots. Then, a coordinate transformation is applied to express the multi-robot model in terms of formation states, which can be selected as: the relative positions between robots, the formation position, the formation heading, etc. The technique of inverse dynamics is applied to this multi-robot model to design the formation control law. The resulting control law presents as distinctive features the fact that it allows positioning as well as tracking of desired formations. Also, final actuation on the robots is in terms of linear and angular reference velocities, as it is usual in commercial robots. Finally it is noted that this centralized formation controller is based on the complete nonlinear dynamics model of the robot.

The paper is organized as follows. In Section II, the complete dynamic model and its linear parameterization are presented. Section III develops the input-output feedback linearization of the robot model. Section IV presents the formation control and its stability analysis. Section V shows experimental results, and finally, in Section VI, some conclusions and suggestions for future work are given.

II. DYNAMIC MODELING

In this section a unicycle-like mobile robot is considered, which will take part into the multi-robot formation. The unicycle like robot presents the advantage of high mobility, high traction with pneumatic tires, and a simple wheel configuration [18]. Due to these advantages, this robot structure has been utilized in applications such as automating highway maintenance and constructions. The mobile robot is illustrated in Fig. 1, where G is the center of mass; B is the wheel baseline center; $h=[x\ \ y]^{\mathrm{T}}$ is the point that is required to tracks a trajectory; u and $\bar{u}$ are the longitudinal and lateral velocities of the center of mass; ω and ψ are the angular velocity and heading of the robot; d, b, a, e and c are distances; $F_{rrx'}$ and $F_{rry'}$ are the longitudinal and lateral tire forces of the right wheel; $F_{rlx'}$ and $F_{rly'}$ are the longitudinal and lateral tire forces of the left wheel; $F_{cx'}$ and $F_{cy'}$ are the longitudinal and lateral force exerted on C by the castor; $F_{ex'}$ and $F_{ey'}$ are the longitudinal and lateral force exerted on E by the tool; and τ_e is the moment exerted by the tool.

The force and moment equations for the robot are [5]:

$$\sum F_{x'} = m\left(\dot{u}-\bar{u}\omega\right) = F_{rlx'}+F_{rrx'}+F_{ex'}+F_{cx'}\ ,$$
$$\sum F_{y'} = m\left(\dot{\bar{u}}+u\omega\right) = F_{rly'}+F_{rry'}+F_{ey'}+F_{cy'}\ ,$$
$$\sum M_z = I_z\dot{\omega} = \frac{d}{2}\left(F_{rrx'}-F_{rlx'}\right)-b\left(F_{rly'}+F_{rry'}\right)+$$
$$\left(e-b\right)F_{ey'}+\left(c-b\right)F_{cy'}+\tau_e\,; \qquad (1)$$

where m is the robot mass; and I_z is the robot moment of inertia about la vertical axis located in G. The kinematics of point h is:

$$\dot{x} = u\cos\psi-\bar{u}\sin\psi-\left(a-b\right)\omega\sin\psi\,,$$
$$\dot{y} = u\sin\psi+\bar{u}\cos\psi+\left(a-b\right)\omega\cos\psi\,. \qquad (2)$$

According to [18], velocities u, ω and $\bar{u}$, including the slip speeds, are:

$$u = \frac{1}{2}\left[r\left(\omega_r+\omega_l\right)+\left(u_r^s+u_l^s\right)\right],$$
$$\omega = \frac{1}{d}\left[r\left(\omega_r-\omega_l\right)+\left(u_r^s-u_l^s\right)\right],$$
$$\bar{u} = \frac{b}{d}\left[r\left(\omega_r-\omega_l\right)+\left(u_r^s-u_l^s\right)\right]+\bar{u}^s\,, \qquad (3)$$

where r is the right and left wheel radius; ω_r and ω_l are the angular velocities of the right and left wheels; u_r^s and u_l^s are the longitudinal slip speeds of the right and left wheel, and $\bar{u}^s$ is the lateral slip speed of the wheels.

The motor models attained by neglecting the voltage on the inductances are:

$$\tau_r = k_a\left(v_r-k_b\omega_r\right)/R_a\,,\ \ \tau_l = k_a\left(v_l-k_b\omega_l\right)/R_a\,. \qquad (4)$$

where v_r and v_l are the input voltages applied to the right and left motors; k_b is equal to the voltage constant multiplied by the gear ratio; R_a is the electric resistance constant; τ_r and τ_l are the right and left motor torques multiplied by the gear ratio; and k_a is the torque constant multiplied by the gear ratio. The dynamic equations of the motor-wheels are:

$$I_e\dot{\omega}_r+B_e\omega_r = \tau_r-F_{rrx'}R_t\,,\quad I_e\dot{\omega}_l+B_e\omega_l = \tau_l-F_{rlx'}R_t\,, \qquad (5)$$

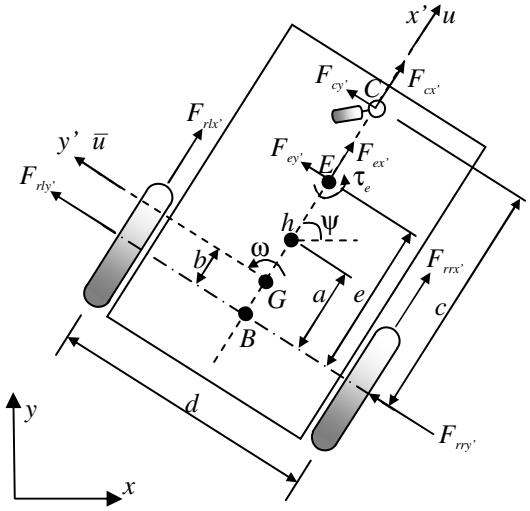

Fig. 1. Parameters of the unicycle-like mobile robot

where I_e and B_e are the moment of inertia and the viscous friction coefficient of the combined motor rotor, gearbox, and wheel, and R_t is the nominal radius of the tire.

In general, most market-available robots have low level PID velocity controllers to track input reference velocities and do not allow the motor voltage to be driven directly. Therefore, it is useful to express the mobile robot model in a suitable way by considering rotational and translational reference velocities as control signals. For this purpose, the velocity controllers are included into the model. To simplify the model, a PD velocity controller has been considered which is described by the following equations:

$$\begin{bmatrix} v_u \\ v_\omega \end{bmatrix} = \begin{bmatrix} k_{PT}\left(u_{ref}-u\right)-k_{DT}\dot{u} \\ k_{PR}\left(\omega_{ref}-\omega\right)-k_{DR}\dot{\omega} \end{bmatrix}. \qquad (6)$$

Variables $\dot{u}_{ref}$ and $\dot{\omega}_{ref}$ are neglected in (6) to further simplify the model.

From (1), (2), (3), (4), (5) and (6) the following dynamic model of the mobile robot is obtained:

$$\begin{bmatrix} \dot{x} \\ \dot{y} \\ \dot{\psi} \\ \dot{u} \\ \dot{\omega} \end{bmatrix} = \begin{bmatrix} u\cos\psi-a\omega\sin\psi \\ u\sin\psi+a\omega\cos\psi \\ \omega \\ \dfrac{\bar{\theta}_3^0}{\bar{\theta}_1^0}\omega^2-\dfrac{\bar{\theta}_4^0}{\bar{\theta}_1^0}u \\ -\dfrac{\bar{\theta}_5^0}{\bar{\theta}_2^0}u\omega-\dfrac{\bar{\theta}_6^0}{\bar{\theta}_2^0}\omega \end{bmatrix} + \begin{bmatrix} 0 & 0 \\ 0 & 0 \\ 0 & 0 \\ \dfrac{1}{\bar{\theta}_1^0} & 0 \\ 0 & \dfrac{1}{\bar{\theta}_2^0} \end{bmatrix} \begin{bmatrix} u_{ref} \\ \omega_{ref} \end{bmatrix} + \begin{bmatrix} \delta_x \\ \delta_y \\ 0 \\ \bar{\delta}_u \\ \bar{\delta}_\omega \end{bmatrix}. \qquad (7)$$

The parameters of the dynamic model are:

$$\bar{\theta}_1^0 = \left(\frac{R_a}{k_a}\left(mR_tr+2I_e\right)+2rk_{DT}\right)/\left(2rk_{PT}\right),$$
$$\bar{\theta}_2^0 = \left(\frac{R_a}{k_a}\left(I_ed^2+2R_tr\left(I_z+mb^2\right)\right)+2rdk_{DR}\right)/\left(2rdk_{PR}\right), \qquad (8)$$

$$\bar{\theta}_3^0 = \frac{R_a}{k_a} mbR_t/(2k_{PT}),\quad \bar{\theta}_4^0 = \frac{R_a}{k_a}\left(\frac{k_a k_b}{R_a} + B_e\right)/(rk_{PT}) + 1,$$
$$\bar{\theta}_5^0 = \frac{R_a}{k_a} mbR_t/(dk_{PR}),\quad \bar{\theta}_6^0 = \frac{R_a}{k_a}\left(\frac{k_a k_b}{R_a} + B_e\right) d/(2rk_{PR}) + 1. \quad (9)$$

The elements of the uncertainty vector $\begin{bmatrix}\delta_x & \delta_y & 0 & \bar{\delta}_u & \bar{\delta}_\omega\end{bmatrix}^T$ are:

$$\delta_x = -\bar{u}^s \sin\psi,$$
$$\delta_y = \bar{u}^s \cos\psi,$$

$$\bar{\delta}_u = \frac{\frac{m\omega\bar{u}^s + F_{ex'} + F_{cx'}}{I_e} + \left(\frac{k_a k_b}{R_a} + B_e\right)\frac{u_r^s + u_l^s}{R_t r I_e} + \frac{\dot{u}_r^s + \dot{u}_l^s}{R_t r}}{\frac{m}{I_e} + \frac{2}{R_t r} + \frac{2k_{DT}k_a}{R_a R_t I_e}},$$

$$\bar{\delta}_\omega = \frac{\left(\frac{k_a k_b}{R_a} + B_e\right)\frac{u_r^s - u_l^s}{2R_t r I_e} + \frac{\dot{u}_r^s - \dot{u}_l^s}{2R_t r} - \frac{mb\dot{\bar{u}}^s}{I_e d} + \frac{eF_{ey'} + cF_{cy'} + \tau_e}{I_e d}}{\frac{d}{2R_t r} + \frac{I_z + mb^2}{I_e d} + \frac{k_{DR}k_a}{R_t R_a I_e}}.$$

The uncertainty vector in (7) will not be considered, if the slip speed of the wheels, the forces and moments exerted by the tool, and the forces exerted by the castor are of no significant value.

Accelerations $\dot{u}$ and $\dot{\omega}$ do not depend on the states ψ, x and y; then $\dot{u}$ and $\dot{\omega}$ can be expressed as follows:

$$\begin{bmatrix}\dot{u}\\ \dot{\omega}\end{bmatrix} = \begin{bmatrix}\frac{\bar{\theta}_3^0}{\bar{\theta}_1^0}\omega^2 - \frac{\bar{\theta}_4^0}{\bar{\theta}_1^0}u + \frac{1}{\bar{\theta}_1^0}u_{ref}\\ -\frac{\bar{\theta}_5^0}{\bar{\theta}_2^0}u\omega - \frac{\bar{\theta}_6^0}{\bar{\theta}_2^0}\omega + \frac{1}{\bar{\theta}_2^0}\omega_{ref}\end{bmatrix} + \begin{bmatrix}\bar{\delta}_u\\ \bar{\delta}_\omega\end{bmatrix}.$$

By re-arranging -and disregarding the uncertainty vector- the linear parameterization of (10) is attained:

$$\begin{bmatrix}\dot{u} & 0 & -\omega^2 & u & 0 & 0\\ 0 & \dot{\omega} & 0 & 0 & u\omega & \omega\end{bmatrix}\bar{\theta}^0 = \begin{bmatrix}u_{ref}\\ \omega_{ref}\end{bmatrix}, \quad (10)$$

where $\bar{\theta}^0 = \begin{bmatrix}\bar{\theta}_1^0 & \bar{\theta}_2^0 & \bar{\theta}_3^0 & \bar{\theta}_4^0 & \bar{\theta}_5^0 & \bar{\theta}_6^0\end{bmatrix}^T$. With an identification method, $\bar{\theta}^0$ can be easily identified.

III. INPUT-OUTPUT FEEDBACK LINEARIZATION OF THE MODEL

In order to perform the input-output feedback linearization of model (7), the output vector is defined as:

$$h = \begin{bmatrix}x\\ y\end{bmatrix}. \quad (11)$$

Considering model (7), the first and second time derivatives of (11) can be expressed as:

$$\dot{h} = \begin{bmatrix}\dot{x}\\ \dot{y}\end{bmatrix} = \begin{bmatrix}u\cos\psi - a\omega\sin\psi\\ u\sin\psi + a\omega\cos\psi\end{bmatrix} + \begin{bmatrix}\delta_x\\ \delta_y\end{bmatrix}, \quad (12)$$

$$\ddot{h} = \begin{bmatrix}-u\omega\sin\psi - a\omega^2\cos\psi\\ u\omega\cos\psi - a\omega^2\sin\psi\end{bmatrix} + \begin{bmatrix}\cos\psi & -a\sin\psi\\ \sin\psi & a\cos\psi\end{bmatrix}\times$$
$$\left(\begin{bmatrix}\frac{\bar{\theta}_3^0}{\bar{\theta}_1^0}\omega^2 - \frac{\bar{\theta}_4^0}{\bar{\theta}_1^0}u\\ -\frac{\bar{\theta}_5^0}{\bar{\theta}_2^0}u\omega - \frac{\bar{\theta}_6^0}{\bar{\theta}_2^0}\omega\end{bmatrix} + \begin{bmatrix}\frac{1}{\bar{\theta}_1^0} & 0\\ 0 & \frac{1}{\bar{\theta}_2^0}\end{bmatrix}\begin{bmatrix}u_{ref}\\ \omega_{ref}\end{bmatrix}\right) + \eta, \quad (13)$$

where:

$$\eta = \begin{bmatrix}\cos\psi & -a\sin\psi\\ \sin\psi & a\cos\psi\end{bmatrix}\begin{bmatrix}\bar{\delta}_u\\ \bar{\delta}_\omega\end{bmatrix} + \begin{bmatrix}\dot{\delta}_x\\ \dot{\delta}_y\end{bmatrix}.$$

From (12) and (13), it can be noted that the system has a total relative degree equal to 4. Considering (13) the following control input is obtained:

$$\begin{bmatrix}u_{ref}\\ \omega_{ref}\end{bmatrix} = \begin{bmatrix}\bar{\theta}_1^0 & 0\\ 0 & \bar{\theta}_2^0\end{bmatrix}\left(\begin{bmatrix}\cos\psi & \sin\psi\\ -\frac{1}{a}\sin\psi & \frac{1}{a}\cos\psi\end{bmatrix}\times\right.$$
$$\left.\left(\upsilon - \begin{bmatrix}-u\omega\sin\psi - a\omega^2\cos\psi\\ u\omega\cos\psi - a\omega^2\sin\psi\end{bmatrix}\right) - \begin{bmatrix}\frac{\bar{\theta}_3^0}{\bar{\theta}_1^0}\omega^2 - \frac{\bar{\theta}_4^0}{\bar{\theta}_1^0}u\\ -\frac{\bar{\theta}_5^0}{\bar{\theta}_2^0}u\omega - \frac{\bar{\theta}_6^0}{\bar{\theta}_2^0}\omega\end{bmatrix}\right), \quad (14)$$

where υ is the new input, which is defined in the formation control design. Equation (14) is constrained to a nonzero value of a. Substituting (14) into (13), the input-output feedback linearized system can be expressed as

$$\ddot{h} = \upsilon + \eta. \quad (15)$$

The following inequality is obtained from (12):

$$|\omega| \le |1/a| C_{h\delta}, \quad \text{where } C_{h\delta} = \max\left(\left\|\dot{h}\right\|\right) + \max\left(\left|\bar{u}^s\right|\right).$$

Let ω_{max} be the saturation value of $|\omega|$. Then, to avoid the saturation of ω, the following condition must be met:

$$|a| \ge C_{h\delta}/\omega_{max}. \quad (16)$$

In order to find the internal dynamics, the following map is considered [11]:

$$\gamma = \Gamma(X) = \begin{bmatrix}x\\ y\\ u\cos\psi - a\omega\sin\psi\\ u\sin\psi + a\omega\cos\psi\\ \psi\end{bmatrix}, \quad (17)$$

where $X = \begin{bmatrix}x & y & \psi & u & \omega\end{bmatrix}^T$. This map defines a diffeomorphism whose inverse is:

$$X = \Gamma^{-1}(\gamma) = \begin{bmatrix}\gamma_1\\ \gamma_2\\ \gamma_5\\ \gamma_3\cos\gamma_5 + \gamma_4\sin\gamma_5\\ -\frac{1}{a}\gamma_3\sin\gamma_5 + \frac{1}{a}\gamma_4\cos\gamma_5\end{bmatrix}. \quad (18)$$

where γ_i is the i-th element of vector γ.

The input-output feedback linearized model expressed in the new coordinates is:

$$\dot{\gamma} = \begin{bmatrix} \gamma_3 + \delta_x \\ \gamma_4 + \delta_y \\ \upsilon_1 + \eta_1 - \dot{\delta}_x \\ \upsilon_2 + \eta_2 - \dot{\delta}_y \\ -\frac{1}{a}\gamma_3 \sin\gamma_5 + \frac{1}{a}\gamma_4 \cos\gamma_5 \end{bmatrix}. \quad (19)$$

where υ_i is the *i*-th element of vector υ; and η_i is the *i*-th element of vector η. From (19) the internal dynamics is obtained:

$$\dot{\gamma}_5 = -\frac{1}{a}\gamma_3 \sin\gamma_5 + \frac{1}{a}\gamma_4 \cos\gamma_5, \quad (20)$$

which is unobservable and uncontrollable. From (17), $\gamma_5=\psi$ is attained. Analyzing ψ in (7) and in (14), it can be concluded that it is not necessary to bound this angle. However, $\dot{\gamma}_5 = \dot{\psi} = \omega$ needs to be bounded. The following analysis proves the boundedness of $\dot{\gamma}_5$:

$$|\dot{\gamma}_5| = \left| -\frac{1}{a}\gamma_3 \sin\gamma_5 + \frac{1}{a}\gamma_4 \cos\gamma_5 \right| \le \left|\frac{1}{a}\right| \left(|\gamma_3| + |\gamma_4| \right). \quad (21)$$

The formation control of section IV guarantees that $\dot{x} \to \dot{x}_d$ or at least $\dot{x}$ gets into a neighborhood of $\dot{x}_d$, then:

$$|\dot{x} - \dot{x}_d| \le C_{xpe}, \quad (22)$$

where C_{xpe} is a bound of $|\dot{x} - \dot{x}_d|$. From (12) and (17), $\gamma_3 = \dot{x} - \dot{\delta}_x$ is obtained. Then, a bound of $|\gamma_3|$ is calculated as follows:

$$|\gamma_3| = |\dot{x} - \delta_x - \dot{x}_d + \dot{x}_d| \le |\dot{x} - \dot{x}_d| + |\dot{x}_d| + |\delta_x|,$$
$$|\gamma_3| \le C_{xpe} + C_{xpd} + C_{\delta x} = C_{\gamma 3}, \quad (23)$$

where C_{xpd} is a bound of $|\dot{x}_d|$; and C_{δ_x} is a bound of $|\delta_x|$. Similarly, a bound of $|\gamma_4|$ can be calculated:

$$|\gamma_4| \le C_{ype} + C_{ypd} + C_{\delta y} = C_{\gamma 4}, \quad (24)$$

where C_{ype} is a bound of $|\dot{y} - \dot{y}_d|$; C_{ypd} is a bound of $|\dot{y}_d|$; and C_{δ_y} is a bound of $|\delta_y|$. Using (23) and (24) in (21):

$$|\dot{\gamma}_5| \le \left|\frac{1}{a}\right| \left(|\gamma_3| + |\gamma_4| \right) \le \left|\frac{1}{a}\right| \left(C_{\gamma 3} + C_{\gamma 4} \right). \quad (25)$$

Then, it can be concluded that $\dot{\gamma}_5 = \dot{\psi} = \omega$ is bounded and the internal dynamics (20) shows a good behavior.

IV. FORMATION CONTROL

The input-output feedback linearized model of the *i*-th mobile robot in a multi-robot system is defined as:

$$\ddot{h}^i = \upsilon^i + \eta^i.$$

Then, the model of the multi-robot system with *n* mobile robots is:

$$\ddot{\xi} = \mu + \Pi, \quad (26)$$

where $\xi = \left[\left(h^1\right)^T \ \ldots \ \left(h^n\right)^T \right]^T$, $\mu = \left[\left(\upsilon^1\right)^T \ \ldots \ \left(\upsilon^n\right)^T \right]^T$, and $\Pi = \left[\left(\eta^1\right)^T \ \ldots \ \left(\eta^n\right)^T \right]^T$. The elements of ξ and $\dot{\xi}$ are considered the system states.

A variable z^1 is defined as the vector that contains the formation parameters: relative positions between robots, centroid position, formation heading, etc. A variable z^2 is defined as the time derivative of z^1, thus $z^2 = \dot{z}^1$. A coordinate transformation is performed in order to express the multi-robot system model (26) in terms of the formation state vector $z=[(z^1)^T \ (z^2)^T]^T$. To this aim, a smooth map ϕ_1 is defined that associates ξ with z^1, such that it has a smooth inverse ϕ_1^{-1}. Now, a map ϕ is defined in terms of ϕ_1 that associates the state vector $[\xi^T \ \dot{\xi}^T]^T$ with the formation state vector z:

$$\begin{bmatrix} z^1 \\ z^2 \end{bmatrix} = \begin{bmatrix} \phi_1(\xi) \\ J(\xi)\dot{\xi} \end{bmatrix} = \phi(\xi, \dot{\xi}), \quad \text{where } J(\xi) = \frac{\partial \phi_1(\xi)}{\partial \xi}. \quad (27)$$

This map defines a diffeomorphism which inverse is:

$$\begin{bmatrix} \xi \\ \dot{\xi} \end{bmatrix} = \begin{bmatrix} \phi_1^{-1}(z^1) \\ \bar{J}(z^1) z^2 \end{bmatrix} = \phi^{-1}(z), \text{ where } \bar{J}(z^1) = \frac{\partial \phi_1^{-1}(z^1)}{\partial z^1}. \quad (28)$$

From (28), the time derivative of $\dot{\xi}$ is:

$$\ddot{\xi} = \frac{d\left(\bar{J}(z^1) z^2\right)}{dt} = \dot{\bar{J}}(z) z^2 + \bar{J}(z^1) \dot{z}^2. \quad (29)$$

By substituting (26) into (29) the new representation of the multi-robot system is obtained:

$$\dot{z}^2 = -\bar{J}(z^1)^{-1} \dot{\bar{J}}(z) z^2 + \bar{J}(z^1)^{-1} \mu + \bar{J}(z^1)^{-1} \Pi. \quad (30)$$

The following inverse dynamics formation control law is proposed:

$$\mu = \bar{J}(z^1)\left(K_1 \tilde{z}^1 + K_2 \tilde{z}^2 + \dot{z}^2_d \right) + \dot{\bar{J}}(z) z^2, \quad (31)$$

where $\tilde{z}^1 = z^1{}_d - z^1$; $\tilde{z}^2 = z^2{}_d - z^2$; $z^2{}_d = \dot{z}^1_d$; $z_d=[(z^1{}_d)^T \ (z^2{}_d)^T]^T$ is the desired formation state vector; $K_1>0$; and $K_2>0$. Then, the closed loop system obtained by substituting the controller of (31) into the system model of (30) is:

$$-\bar{J}(z^1)^{-1} \Pi = K_1 \tilde{z}^1 + K_2 \tilde{z}^2 + \dot{\tilde{z}}^2. \quad (32)$$

which can be expressed as:

$$\dot{\tilde{z}} = A_z \tilde{z} - \begin{bmatrix} 0 & \bar{\Pi}^T \end{bmatrix}^T, \quad (33)$$

where $\bar{\Pi} = \bar{J}(z^1)^{-1} \Pi$; $\tilde{z} = \left[\left(\tilde{z}^1\right)^T \ \left(\tilde{z}^2\right)^T \right]^T = z_d - z$; and:

$$A_z = \begin{bmatrix} 0 & I_{2n\times 2n} \\ -K_1 & -K_2 \end{bmatrix}. \quad (34)$$

In (34), $I_{2n\times 2n}$ represents the $2n\times 2n$ identity matrix. Let consider K_1 and K_2 as diagonal matrices with positive elements different from zero. From these considerations, A_z is Hurwitz.

The following Lyapunov candidate and its time derivative are now considered:

$$V(\tilde{z}) = \tilde{z}^T P \tilde{z} > 0; \quad P = P^T > 0$$
$$\dot{V}(\tilde{z}) = -\tilde{z}^T Q \tilde{z} - 2\tilde{z}^T P \begin{bmatrix} 0 & \bar{\Pi}^T \end{bmatrix}^T \tag{35}$$

where:

$$Q = -\mathrm{A}_z^T P - P\mathrm{A}_z \tag{36}$$

Matrix Q is chosen as $Q=I_{4n\times 4n}$, where $I_{4n\times 4n}$ is the $4n\times 4n$ identity matrix. Matrix P is calculated from (36). Since A_z is Hurwitz, $P=P^T>0$. A sufficient condition for the second of (35) to be negative definite is:

$$\|\tilde{z}\| > 2\left\| P \begin{bmatrix} 0 & \bar{\Pi}^T \end{bmatrix}^T \right\| \tag{37}$$

If vector $\bar{\Pi}$ is bounded, the formation error vector $\tilde{z}$ will also be bounded after a finite time. If the uncertainty vectors of the robots are null, then $\bar{\Pi}=0$ and $z \to z_d$ with $t \to \infty$.

Remark 1. The proposed controller is able to track a moving or continuously varying desired formation.

Remark 2. The controller needs either the sensorial information from the direct measurement of formation state vector z or the calculation of these states by measuring the state vector $[\xi^T \ \dot{\xi}^T]^T$. In the last case, equation (27) has to be used to be replaced into the control law (31). If necessary, the following equations -obtained from (27) and (28)- can be used as well:

$$\bar{J}(z^1) = J(\xi)^{-1}, \quad \dot{\bar{J}}(z) z^2 = -J(\xi)^{-1} \dot{J}(\xi, \dot{\xi}) \dot{\xi}. \tag{38}$$

Remark 3. $\phi^{-1}(z) \to \phi^{-1}(z_d)$ with $z \to z_d$ because $\phi^{-1}(.)$ is a continuous function. Therefore, from (28) $\xi \to \xi_d$ and $\dot{\xi} \to \dot{\xi}_d$ with $z \to z_d$, where $\begin{bmatrix} \xi_d^T & \dot{\xi}_d^T \end{bmatrix}^T = \phi^{-1}(z_d)$.

V. EXPERIMENT

An experiment to test the control of a two-robot formation was performed using two Pioneer mobile robots, one of which had an omnidirectional camera system and an on-board computer to monitor and control the other robot (see Fig. 2).

The identification of the robot model was performed by using least squares estimation [2] applied to a filtered regression model [13] obtained from (10). The identified parameters of the robot with the omnidirectional camera system are:

$$\bar{\theta}_1^0 = 0.26038, \quad \bar{\theta}_2^0 = 0.25095, \quad \bar{\theta}_3^0 = -0.00049969,$$
$$\bar{\theta}_4^0 = 0.99646, \quad \bar{\theta}_5^0 = 0.002629, \quad \bar{\theta}_6^0 = 1.0768.$$

In (16), $C_{h\delta}$=0.2m/s and ω_{max}=1.745rad/s are considered, thus $|a| \geq 0.1146$m. Then, a constant a=0.12m was chosen.

The formation states were defined as: d_{12}, x_1, y_1, θ_c (see Fig. 3) and its derivatives; and desired values were defined as: d_{12d}, x_{1d}, y_{1d} and θ_{cd}. Map ϕ_1 is defined as follows:

$$z^1 = \begin{bmatrix} d_{12} \\ x_1 \\ y_1 \\ \theta_c \end{bmatrix} = \phi_1(\xi) = \begin{bmatrix} \sqrt{(x_2 - x_1)^2 + (y_2 - y_1)^2} \\ x_1 \\ y_1 \\ f_\zeta(x_1 - x_2, y_1 - y_2) \end{bmatrix}. \tag{39}$$

In (39), x_i, y_i are elements of the vector h^i; function $f_\zeta(x,y)$ allows calculating the angle of the vector (x,y). This angle lies in the range $[\zeta, 2\pi+\zeta)$. For instance $f_\zeta(x,y)$=atan2(y,x) when $\zeta=-\pi$.

The inverse map ϕ_1^{-1} is calculated as follows:

$$\xi = \begin{bmatrix} x_1 \\ y_1 \\ x_2 \\ y_2 \end{bmatrix} = \phi_1^{-1}(z^1) = \begin{bmatrix} x_1 \\ y_1 \\ x_1 - d_{12}\cos(\theta_c) \\ y_1 - d_{12}\sin(\theta_c) \end{bmatrix}. \tag{40}$$

Map ϕ_1 defines the diffeomorphism ϕ of (27) in the region $\Omega = \mathbb{R}^8$.

From (28), the Jacobian $\bar{J}(z)$ is calculated as:

$$\bar{J}(z^1) = \begin{bmatrix} 0 & 1 & 0 & 0 \\ 0 & 0 & 1 & 0 \\ -\cos\theta_c & 1 & 0 & d_{12}\sin\theta_c \\ -\sin\theta_c & 0 & 1 & -d_{12}\cos\theta_c \end{bmatrix}. \tag{41}$$

The following control parameters are used in the experiment:

$$K_1 = diag(0.36,\ 0.25,\ 0.25,\ 0.25),$$
$$K_2 = diag(1.2,\ 1,\ 1,\ 1), \quad \zeta = 0,$$

Fig. 2. Mobile robots and omnidirectional camera

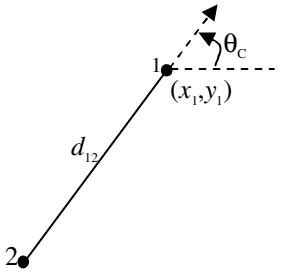

Fig. 3. Formation variables

where *diag(.)* represents a diagonal matrix. The initial velocities of the robots are set to zero. The desired formation is chosen as:

$$z^1{}_d = \begin{bmatrix} 1.2 & 0.5+0.05t & 0 & \pi \end{bmatrix}^T$$
$$z^2{}_d = \begin{bmatrix} 0 & 0.05 & 0 & 0 \end{bmatrix}^T .$$

In z_d, the positions and distances are expressed in meters and the angles are in radians.

Figures 4 and 5 present the experimental results of the formation control, showing a good tracking performance of the desired formation. The formation errors are smaller than 0.05m (distance errors) and smaller than 0.03rad (angle error) after 17.5 seconds. These results validate the theoretical controller design presented in the previous sections.

VI. CONCLUSION

A complete dynamic model of a unicycle-like mobile robot and its linear parameterization were presented. An input-output feedback linearization of the model was performed. Then, after defining a formation state vector, a formation control of the multi-robot system was designed using inverse dynamics. The controller allows the tracking of desirable formations evolving on the plane. The use of the formation states, both in the model and in the formation control design of the multi-robot system, allows achieving a better design of the time evolution of the formation.

Future work will delve into the issues of obstacle avoidance and decentralized formation control.

REFERENCES

[1] G. Antonelli and S. Chiaverini, "Kinematic Control of a Platoon of Autonomous Vehicles", *IEEE International Conference on Robotics and Automation*, Taipei, Taiwan, September 2003, pp. 1464-1469.

[2] K. J. Aström and B. Wittenmark, *Adaptive control,* Addison-Wesley, 1995.

[3] T. Balch and R. C. Arkin, "Behavior-based formation control for multirobot teams," *IEEE Transactions on Robotics and Automation*, vol. 14, no. 6, pp. 926-939, December 1998.

[4] C. Belta and V. Kumar, "Trajectory design for formations of robots by kinetic energy shaping," *IEEE International Conference on Robotics and Automation*, Washington, DC, May 2002, pp. 2593-2598.

[5] F. D. Boyden and S. A. Velinsky, "Dynamic Modeling of Wheeled Mobile Robots for High Load Applications," *IEEE International Conference on Robotics and Automation*, vol. 4, pp. 3071-3078, 1994.

[6] A. K. Das, et al., "A vision-based formation control framework," *IEEE Transactions on Robotics and Automation*, vol. 18, no. 5, pp. 813-825, October 2002.

[7] J. P. Desai, J. Ostrowski, and V. Kumar, "Controlling formations of multiple mobile robots," *in Proc. IEEE Int. Conf. Robotics and Automation*, Leuven, Belgium, May 1998, pp. 2864-2869.

[8] R. Fierro, A. K. Das, V. Kumar, and J. P. Ostrowski, "Hibrid control of formations of robots," *in Proc. IEEE Int. Conf. Robotics and Automation*, Seoul, Korea, May 2001, pp. 3672-3677.

[9] J. Fredslund and M. J. Mataric, "Robot formations using only local sensing and control," *IEEE International Symposium on Computational Intelligence in Robotics and Automation*, Banff, Alberta, Canada, July 2001, pp. 308-313.

[10] R. Kelly, R. Carelli, J. M. Ibarra Zannatha, and C. Monroy, "Control de una pandilla de robots móviles para el seguimiento de una constelación de puntos objetivo," *VI Congreso Mexicano de Robótica*, COMRob, Torreón, Coahuila, Mexico, October 2004.

[11] J. R. T. Lawton, R. W. Beard, and B. J. Young, "A Decentralized Approach to Formation Maneuvers," *IEEE Transactions on Robotics and Automation*, vol. 19, no. 6, pp. 933-941, December 2003.

[12] S. Monteiro, M. Vaz, and E. Bicho, "Attractor dynamics generates robot formations: from theory to implementation," *IEEE International Conference on Robotics and Automation*, New Orleans, LA, April 2004, pp. 2582-2587.

[13] F. Reyes and R. Kelly, "On Parameter Identification of Robot Manipulator," *IEEE International Conference on Robotics and Automation*, Albuquerque, New Mexico, April 1997, pp. 1910-1915.

[14] J. –J. Slotine and W. Li, *Applied nonlinear control*, Prentice Hall Int., 1991.

[15] D. J. Stilwell and B. E. Bishop, "A strategy for controlling autonomous robot platoons", *IEEE Conference on Decision and Control*, Sydney, Australia, December 2000, pp. 3483-3488.

[16] K. H. Tan and M. A. Lewis, "Virtual Structures for High-Precision Cooperative Mobile Robotic Control," *International Conference on Intelligent Robots and Systems*, vol. 1, pp. 132-139, November 1996.

[17] H. Yamaguchi, T. Arai, and G. Beni, "A distributed control scheme for multiple robotic vehicles to make group formations," *Robotics and Autonomous Systems*, vol. 36, pp. 125-147, 2001.

[18] Y. Zhang, D. Hong, J. H. Chung, and S. A. Velinsky, "Dynamic Model Based Robust Tracking Control of a Differentially Steered Wheeled Mobile Robot," *Proceedings of the American Control Conference*, Philadelphia, Pennsylvania, June 1998, pp. 850-855.

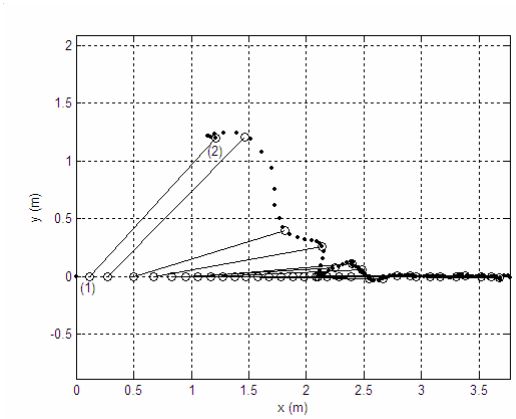

Fig. 4. Formation trajectory, the little circles represent the positions of the robots.

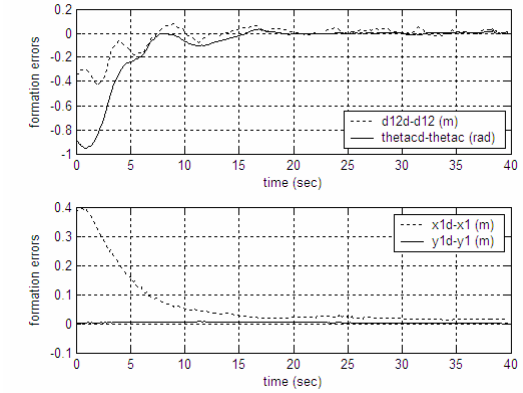

Fig. 5. Formation error through time.